Received: 12 February 2022 | Accepted: 5 June 2022

DOI: 10.1002/jmv.27927

RESEARCH ARTICLE

JOURNAL OF MEDICAL VIROLOGY WILEY

Omicron (BA.1) and sub-variants (BA.1.1, BA.2, and BA.3) of SARS-CoV-2 spike infectivity and pathogenicity: A comparative sequence and structural-based computational assessment

Suresh Kumar[1] | Kalimuthu Karuppanan[2] | Gunasekaran Subramaniam[3]

[1]Department of Diagnostic & Allied Health Science, Faculty of Health and Life Sciences, Management and Science University, Shah Alam, Selangor, Malaysia

[2]Division of Cardiovascular Medicine, Radcliffe Department of Medicine, Wellcome Centre for Human Genetics, University of Oxford, Oxford, UK

[3]Department of Physiology, Anatomy and Genetics, University of Oxford, Oxford, UK

Correspondence

Suresh Kumar, Department of Diagnostic & Allied Health Science, Faculty of Health and Life Sciences, Management and Science University, Seksyen 13, 40100 Shah Alam, Selangor, Malaysia.
Email: sureshkumar@msu.edu.my

Abstract

The Omicron variant of the severe acute respiratory syndrome coronavirus 2 (SARS-CoV-2) has now spread throughout the world. We used computational tools to assess the spike infectivity, transmission, and pathogenicity of Omicron (BA.1) and sub-variants (BA.1.1, BA.2, and BA.3) in this study. BA.1 has 39 mutations, BA.1.1 has 40 mutations, BA.2 has 31 mutations, and BA.3 has 34 mutations, with 21 shared mutations between all. We observed 11 common mutations in Omicron's receptor-binding domain (RBD) and sub-variants. In pathogenicity analysis, the Y505H, N786K, T95I, N211I, N856K, and V213R mutations in omicron and sub-variants are predicted to be deleterious. Due to the major effect of the mutations characterizing in the RBD, we found that Omicron and sub-variants had a higher positive electrostatic surface potential. This could increase interaction between RBD and negative electrostatic surface potential human angiotensin-converting enzyme 2 (hACE2). Omicron and sub-variants had a higher affinity for hACE2 and the potential for increased transmission when compared to the wild-type (WT). Negative electrostatic potential of N-terminal domain (NTD) of the spike protein value indicates that the Omicron variant binds receptors less efficiently than the WT. Given that at least one receptor is highly expressed in lung and bronchial cells, the electrostatic potential of NTD negative value could be one of the factors contributing to why the Omicron variant is thought to be less harmful to the lower respiratory tract. Among Omicron sub-lineages, BA.2 and BA.3 have a higher transmission potential than BA.1 and BA.1.1. We predicted that mutated residues in BA.1.1 (K478), BA.2 (R400, R490, and R495), and BA.3 (R397 and H499) formation of new salt bridges and hydrogen bonds. Omicron and sub-variant mutations at Receptor-binding Motif (RBM) residues such as Q493R, N501Y, Q498, T478K, and Y505H all contribute significantly to binding affinity with human ACE2. Interactions with Omicron variant mutations at residues 493, 496, 498, and 501 seem to restore ACE2 binding effectiveness lost due to other mutations like K417N.

KEYWORDS
BA.1, BA.2, BA.3, BA1.1, COVID-19, Omicron, SARS-CoV-2

1 | INTRODUCTION

The SARS-CoV-2 RNA genome has been rapidly developing since the first epidemic in late 2019.[1] This is mostly due to the virus's polymerase, which is inherently prone to mistakes, and host immune system selection factors. Many concerns about different mutations in the spike protein surfaced in the previous year. On November 26, 2021, the World Health Organization (WHO) classified Omicron as a variant of concern (VOC) after it was discovered in Botswana. The Omicron variant does have more mutations than prior variants, with many of them occurring in the spike protein's receptor-binding domain (RBD).[2] Despite the spread of several COVID-19 waves over the world, no variant has accumulated mutations or allowed immune evasion to the extent that the SARS-CoV-2 Omicron (B.1.1.529) variant has. The Omicron variant has more than 50 mutations, including 26–32 amino acid substitutions, deletions, and insertions.[3,4] The pandemic response strategy for COVID-19 is dependent on the development of treatment options and vaccine formulations.[5–8] Numerous Omicron mutations, on the other hand, have not been discovered in prior VOCs, and their functional implications have not been thoroughly investigated. However, the discovery of multiple unidentified Omicron mutations inside dominant antibody epitopes has raised worries that vaccination and therapeutic antibody effectiveness may be drastically diminished, necessitating new strategic considerations and research objectives.

A lineage is a set of closely related variations that share a common ancestor, and these may then branch off into sub-lineages, as seems to be occurring with Omicron. The Omicron variant is considered to have been divided into four sub-lineages —BA.1, BA.1.1, BA.2, and BA.3[9] which will continue to change in the future. All four lineages were discovered in South Africa at around the same time and location. While all four lineages have expanded worldwide, their rates of spread have varied. This is most certainly owing to differences in the spike protein, which is necessary for viral replication and host cell penetration.

Several Omicron lineages have been found after B.1.1.529 was designated as a VOC on November 26, 2021. Pango lineages BA.1/B.1.1.529.1, BA.1.1/B.1.1.529.1.1, BA.2/B.1.1.529.2, and BA.3/B.1.1.529.3 are among those being monitored by WHO under the "Omicron" umbrella, based on the PANGOLIN (Phylogenetic Assignment of Named Global Outbreak Lineages). According to the outbreak.info website, the cumulative prevalence (the ratio of sequences containing lineage to all sequences submitted to GISAID since lineage identification) for BA.1 is 5% (detected in at least 161 countries), BA.1.1 is 17% (detected in at least 161 countries), BA.2 is 9% (detected in at least 163 countries), and BA.3 is less than 0.5% (detected in at least 35 countries) as of May 26, 2022.

It is essential to monitor and study Omicron (BA.1) and its sub-lineages BA.1.1, BA.2, and BA.3, with a particular emphasis on BA.2,[10] for transmissibility, immunological escape qualities, and virulence, which should be prioritized separately and in contrast to BA.1. In our previous study, we compared Omicron (BA.1) and Delta variants of SARS-CoV-2.[11] In this study, we compared Omicron variants of BA.1, BA.1.1, BA.2, and BA.3 through computational studies. We studied the sequence and structural characterization of the spike protein which is necessary for viral transmission and entry in these four Omicron variant lineages.

2 | METHODOLOGY

2.1 | Omicron and sub-variants protein sequence retrieval

The FASTA sequence for the Wuhan-HU-1 spike protein was obtained from Uniprot[12] (P0DTC2), the protein sequence for BA.2 was obtained from NCBI Genbank[13] (UFO69279.1). BA.1.1 (EPI ISL 7605591) and BA.3 (EPI ISL 9092427) genome sequences were retrieved from GSAID[14] and translated to protein sequences using the Expasy translate tool. The spike protein sequence for BA.1.1 and BA.3 was selected from the translated protein sequence.

2.2 | Multiple alignment of Omicron variants with wild-type

Using Clustal Omega[15] with the default settings, the protein sequence of Wuhan-Hu-1 (wild-type [WT]) was aligned with the protein sequences of omicron variant and sub-lineages BA.1, BA.1.1, BA.2, and BA.3. Based on the multiple alignment, mutations were identified. The alignment figure was prepared using Espirt.

2.3 | Physiochemical characterization

Using the Expasy protparam,[16] the protein sequences of BA.1, BA.1.1, BA.2, and BA.3's whole spike protein and receptor-binding domain (RBD) were compared to Wuhan-Hu-1 (WT). The number of amino acids, molecular weight, theoretical pI, amino acid composition, charged residues, instability index, aliphatic

index, and grand average of hydropathicity (GRAVY) were all analyzed.

2.4 | Secondary structure and intrinsically disordered prediction

The secondary structure of the Wuhan-Hu-1, Omicron variant (BA.1) and sub-variants (BA.2 and BA.3) were predicted using GOR IV.[17] The Garnier–Osguthorpe–Robson (GOR) program analyses secondary protein structure using information theory and Bayesian statistics. The purpose of utilizing GOR to combine numerous sequence alignments is to obtain information for enhanced secondary structure discrimination. The intrinsically disordered spike protein was predicted using PONDR®VLXT tool.

2.5 | Structural modeling of RBD and structure analysis

The crystal structure of SARS-CoV-2 spike RBD bound with ACE2 of Wuhan-HU-1 was obtained using the Protein Data Bank (PDB; PDB ID: 6M0J).[18] The PDB was utilized to get the cryo-electron microscopy (cryo-EM) structure of the SARS-CoV-2 Omicron (BA.1) spike protein in complex with human ACE2 (refinement of RBD and ACE2; PDB ID:7T9L).[19] The structure of BA.1.1, BA.2, and BA.3 was generated by homology modeling with SWISS-MODEL server[20] with the BA.1 template (PDB:7T9L). Similarly, the N-terminal doman (NTD) of spike protein was modeled using SWSS-MODEL server: WT (PDB ID:7L2C), BA.1 (PDB ID:7TEI), BA.1.1 (PDB ID:7TEI), BA.2 (PDB ID:7TO4), and BA.3 (PDB ID:7WK3). The sequence identity of BA.1.1, BA.2, and BA.3 with template (PDB ID: 7T9l) are 99.50%, 97.01%, and 98.51%, respectively. Missing residues were inserted into both cyro-EM and homology modeled proteins, and energy was minimized using GROMOS96 43B1 forcefield available at the Swiss-PDB viewer to remove residue steric overlaps at the interface. The Ramachandran plot and Errat plot were used to assess the structure of the homology models. To identify topological and structural changes between wild and Omicron (BA.1, BA.1.1, BA.2, and BA.3) proteins, TM-score and RMSD (root mean square deviation) data were obtained using the I-Tasser online service.[21] CASTp 3.0[22] was used to predict protein pockets and cavities. The RBD of Omicron and sub-variants were computed for electrostatic potential using electrostatic potential calculated with the Adaptive Poisson–Boltzmann Solver program implemented in PyMOL.[23]

2.6 | Protein–protein docking and stability analysis of RBD-hACE2

The protein–protein docking was carried out between hACE2 and Omicron variants RBD using Hawkdock[24] and cluspro[24] docking program compared with WT. For point mutation docking analysis Hex[25] docking program was used. We used PDBePISA (PISA) web-based tool to investigate the stability of formation of omicron RBD and hACE2 complex.

2.7 | Pathogenicity analysis

PredictSNP[26] was used to determine the pathogenicity of all mutations. Using the PredictSNP web server, prediction algorithms from programs like MAPP, PolyPhen1 and PolyPhen-2, SIFT, SNAP, and PANTHER were utilized to achieve a consensus pathogenicity score. The degree of high accuracy is high due to the consensus technique.

3 | RESULTS AND DISCUSSION

3.1 | Physio-chemical characterization

Wuhan-Hu-1 (WT) includes 1273 amino acids, while Omicron BA.1, BA.1.1, and BA.2 have 1270 and BA.3 has 1267 amino acids. BA.1, BA.1.1, and BA.2 are three amino acid-deficient compared to Wuhan-Hu-1, and BA.3 is six amino acid-deficient compared to WT. Wuhan-Hu-1 has a molecular weight of 141 178.47, BA.1 has a molecular weight of 141 328.11, BA.1.1 has 141 300.09, BA.2 has a molecular weight of 141 185.78, and BA.3 has a molecular weight of 140 900.61. BA.3 has a lower molecular weight than Wuhan-Hu-1 owing to the absence of six amino acid residues, but BA.2, BA.1.1, and BA.1 have slightly greater molecular weight than Wuhan-Hu-1 despite the absence of three amino acid residues. A pI number more than 7 indicates that the protein is alkaline, whereas a value less than 7 suggests that the protein is acidic. The theoretical pI of WT is 6.24, whereas both BA.1 and BA.1.1 have a theoretical pI of 7.14, BA.2 has a theoretical pI of 7.16, and BA.3 has a theoretical pI of 7.35. Omicron BA.1, BA.1.1, BA.2, and BA.3 are shown to be more alkaline than WT. According to previous studies, the SARS-CoV-2 S protein is somewhat more positively charged than the SARS-CoV protein, which may result in a greater propensity for binding to negatively charged areas of other molecules through nonspecific and selective interactions.[27] According to our data, the WT's expected charged residues (Arg + Lys) are 103, both BA.1 and BA.1.1 anticipated charged residues are 111, BA.2 predicted charged residues are 108, and BA.3's predicted charged residues are 109. We noticed that BA.1, BA.1.1, BA.2, and BA.2 all contain significantly more positively charged amino acids (Arg + Lys) than the WT, which may improve their propensity for binding to negatively charged areas of other molecules such as ACE2. According to the instability index, proteins with a stability score of less than 40 have a stable structure. We observed that all BA.1, BA.1.1, BA.2, and BA.3 (34.21–34.69) are as slight improved stability as compared to WT (33.01).[28] Aliphatic index, a positive factor associated with improved thermostability of proteins, is 84.67 for WT, 84.95 for BA.1, BA.1.1, 84.72 for BA.2, and 85.15 for BA.3, indicating that corroborated its stability over a wide range of temperature regime.

According to recent study,[29] increased Omicron thermal stability may result in increased persistence of Omicron in exposed surroundings, posing a greater risk of transmission among household contacts than the Delta form. Increased stability may facilitate viral attachment to host cells by increasing the efficacy of receptor recognition, but it may impair viral membrane fusion.

The grand average of hydropathicity index (GRAVY) was determined using Kyte and Doolittle's hydropathy values. The hydropathy values range from −2 to +2 for most proteins, with the positively rated proteins being more hydrophobic. GRAVY is projected to be −0.079 for WT, −0.080 for BA.1 and BA.1.1, −0.074 for BA.2, and −0.071 for BA.3, indicating their hydrophilic nature. BA.1 and BA.1.1 were found to be more hydrophilic, whilst BA.2 and BA.3 were found to be less hydrophilic, the presence of more hydrophobic residues which likely to increase pathogenicity of viral protein.[30]

From the amino acid composition compared to the WT (Supporting Information: Table S1), there is an increase in charged residues in the side chains such as Arginine (R) and Lysine (K) in the RBD, which often contributes to the formation of salt bridges[31] in BA.1, BA.1.1, BA.2, and BA.3. When compared to the WT, there is an increase in Asparagine (N) residues in the RBD, which leads to hydrogen bond formation in BA.1, BA.1.1, BA.2, and BA.3. In the RBDs of BA.1, B.A.1.1, BA.2, and BA.3, there is an increase in hydrophobic residues such as phenylalanine (F), Alanine (A), Leucine (L), Proline (P), and leucine (L) compared to the WT, which are typically buried within the protein core. In BA.1.1, RBD there is increase in polar amino acids like Tryptophan (W) which is often at the surface of the protein, Serine (S) which forms hydrogen bond and Valine(V) which are hydrophobic when compared to all sub-lineages.

3.2 | Comparison of Omicron lineages for unique and common shared mutations

From the multiple alignment (Supporting Information: Figure S1) of Omicron and sub-variant with WT and from four-way Venn diagram (Figure 1), it is inferred that there are 39 mutations identified for BA.1, 40 mutations for BA.1.1, 31 mutations for BA.2, and 34 mutations for BA.3. Among four-way comparison between Omicron and sub-variants, BA.1.1 has one unique mutation R346K, and BA.2 has eight unique mutations T19I, L24del (deletion), P25del, P26del, A27S, V213G, T376A, and R408S, and for BA.3 has 1 unique mutation R216del.

There are eight common mutations identified between BA.1.1 and BA.1 which are A67V, ins (insertion) 214EP, R216E, S371L, G496S, T547K, N856K, L981F. There are two common identified mutations between BA.2 and BA.3 which are S371F and D405N. There are 10 common identified mutations between BA.1.1, BA.1, and BA.3 which are H69del, V70del, T95I, V143del, Y144del, Y145del, N211I, L212V, V213R, and G446S. There are 21 common elements identified between all four Omicron and sub-variants which are BA.1.1, BA.1, BA.2, and BA.3 are G142D, G339D, S373P, S375F, K417N, N440K, S477N, T478K, E484A, Q493R, Q498R, N501Y, Y505H, D614G, H655Y, N679K, P681H, N764K, D796Y, Q954H, and N969K. Due to triple mutation at the furin cleavage site, such as H655Y, N679K, and P681H Omicron (BA.1) is reported to be extremely transmissible from previous findings.[32] We observed this triple mutation at the furin cleavage site is common in all sub-variants. There is no commonly shared mutation between BA.1 and BA.2, between BA.1 and BA.3, between BA.1, BA.2, and BA.3, between BA.2, BA.3, and BA.1.1, between BA.3 and BA.1.1, between BA.2 and BA.1.1, between BA.1, BA.2, and BA.1.1.

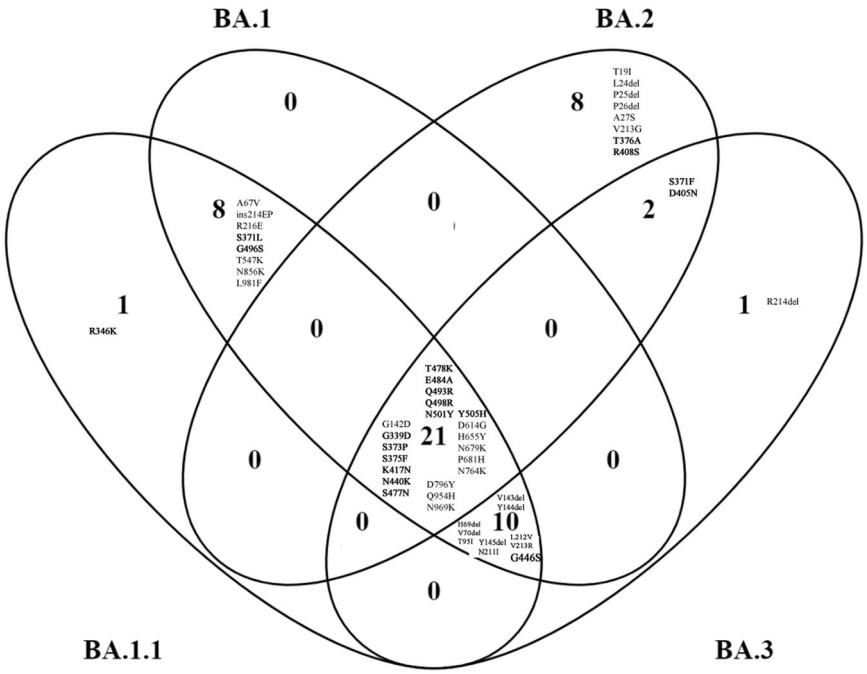

FIGURE 1 Spike protein mutation in Omicron (BA.1) and Omicron sub-variants (BA1.1, BA.2, and BA.3) compared with four-way Venn diagram. Receptor-binding domain (residues 319–541) are marked as bold. Del represents deletion, ins represent insertion.

On three-way comparison between BA.1, BA.2, and BA.3, BA.1 has eight unique mutations A67V, ins214EP, R216E, S371L, G496S, T547K, N856K, and L981F. For BA.2, eight mutations T19I, L24del, P25del, P26del, A27S, V213G, T376A, and R408S. BA.3 has one unique mutation R214del. The shared mutation between BA.1 and BA.3 is H69del, V70del, T95I, V143del, Y144del, Y145del, N211I, L212V, V213R, and G446S. The shared mutation for BA.2 and BA.3 is S371F, D405N. There are 21 common mutations between BA.1, BA.2, and BA.3 which are G142D, G339D, S373P, S375F, K417N, N440K, S477N, T478K, E484A, Q493R, Q498R, N501Y, Y505H, D614G, H655Y, N679K, P681H, N764K, D796Y, Q954H, and N969K.

When we compare BA.1 and BA.2 in two-way comparison, BA.2 has 10 unique mutations T19I, L24del, P25del, P26del, A27S, V213G, S371F, T376A, D405N, and R408S whereas BA.1 has 18 unique mutations A67V, H69del, V70del, T95I, V143del, Y144del, Y145del, N211I, L212V, V213R, ins214EP, R216E, S371L, G446S, G496S, T547K, N856K, and L981F.

In comparison to the RBD (319–541), there are 11 common shared mutations G339D, S373P, S375F, K417N, N440K, S477N, T478K, E484A, Q493R, Q498R, N501Y (Figure 2A–D). Unique mutation for BA.1.1 is R346K, for BA.2 is T376A and R408S. The commonly shared mutation between BA.1 and BA.1.1 is S371L and G496S. Y505H is the commonly shared mutation between BA.1, BA.1.1, and BA.2. G446S is the common mutation between BA.1, BA.1.1, and BA.3. S371F and D405N shared mutations between BA.2 and BA.3. From previous study,[33,34] it is found that neutralizing antibodies in infected patients' sera recognize the RBD (319–541 aa) and the N terminal domain of BA.1 and BA.2 (13–306). The divergence suggests that the sub-variants evolved resistance in different immune pressure, possibly in different hosts. All four Omicron lineages have common mutation at the receptor-binding Motif (RBM) region (437–508a.a) which binds to hACE2 are N440K, S477N, T478K, E484A, Q493R, Q498R, N501Y, and Y505H (Figure 2E). There is one unique mutation at RBM for BA.1 at G446S. According to recent study,[35] during cross-species transmission, SARS-CoV-2 may develop to adapt to a variety of hosts, which inherently favors SARS-CoV-2 evolution. Previously, RBD residues 493, 498, and 501 were identified as key locations for the SARS-CoV-2 host range. Therefore, residues 493, 498, and 501, as well as other changes to omicron's RBD, are likely to alter the host spectrum of SARS-CoV-2, and the possibility of an omicron variant overcoming the species barrier must be examined further in the future.

Previous research has shown that deletion of H69/V70 compensates for immune escape mutations that diminish infectivity; thus, it is critical to keep a check out for deletions that have functional consequences.[36] In contrast to the Omicron BA.1, BA.1.1, and BA.3 spike protein, only the Omicron BA.2 there is absence of the amino acids 69–70 deletion, which is associated with S gene target failure (SGTF) and is not recognized by SGTF.[37] This

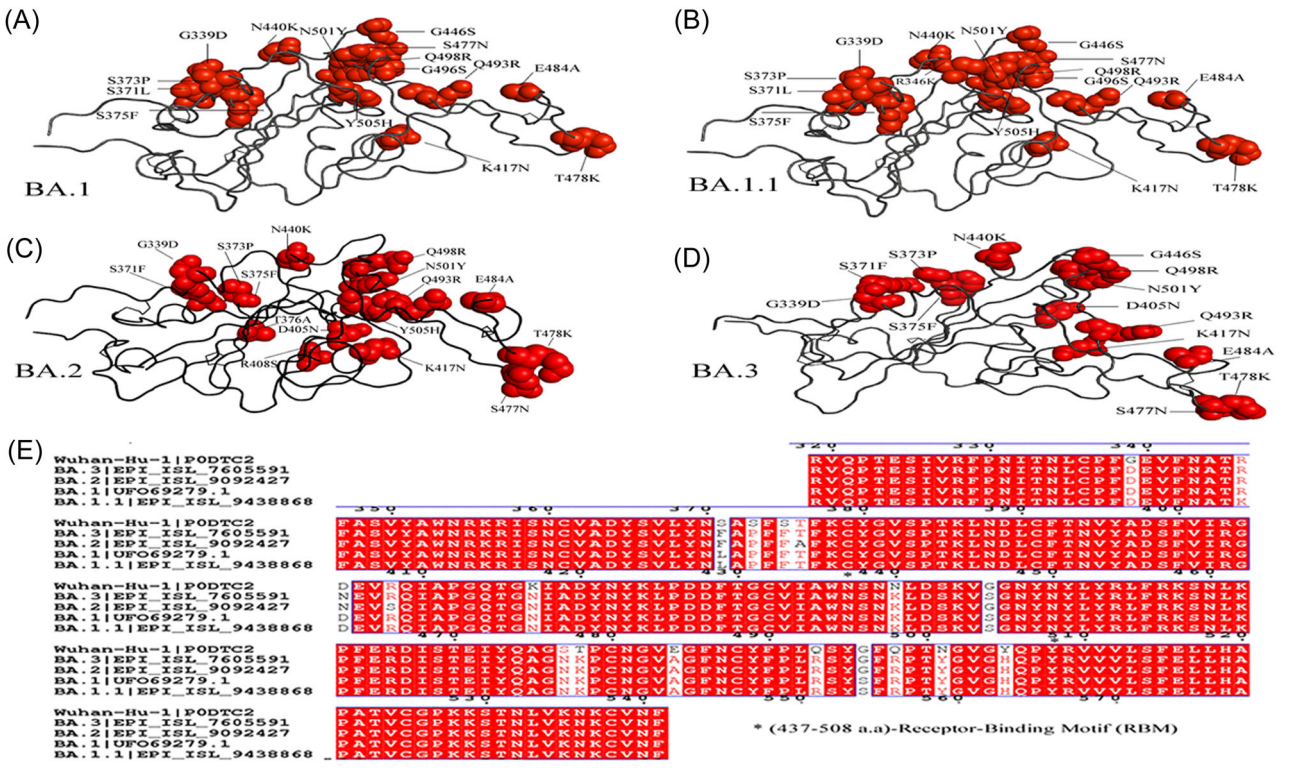

FIGURE 2 Ribbon diagram of the RBD with residue mutated relative to the wild-type (WT). A comparison of (A) Omicron—BA.1, Omicron sub-variants (B) BA.1.1, (C) BA.2, and (D) BA.3 mutation in receptor-binding domain (RBD). The multiple alignment (E) of RBD shows receptor-binding motif (RBM) (residues 437–508) of Omicron variants with WT.

complicates tracking its transmission, and some researchers have dubbed it a "stealth" variant. The N501Y mutation, which enhances receptor binding strength, is found in all four BA.1, BA.1.1, BA.2, and BA.3 proteins, and there is a general positive relationship between the stabilizing effect of mutations on receptor binding and their population incidence.

3.3 | Secondary structure and intrinsically disordered prediction

Through secondary structure prediction (Supporting Information: Table S2), when compared to the WT, Omicron (BA.1, BA.2, and BA.3) entire spike protein and RBD exhibit an increase in alpha-helix and a slight decrease in Extended strand. Only the BA.1.1 lineage contains an increased alpha-helix in the entire spike protein, a decreased RBD, and an increased number of extended-strands; as a result, it has only one unique mutation in comparison to BA.1. The projected rise in alpha-helices shows that alpha helices are more prone to mutations than beta-strands.[38] When compared to the WT, there is a slight decrease in random coil in the total spike protein of all Omicron variants (BA.1) and sub-variants (BA2 and BA.3), while there is a slight increase in random coil in the RBD.[39]

The Omicron variant of spike protein is less disordered than the WT, according to the Intrinsically disordered prediction (Supporting Information: Table S3). There is a disorder to order transition[40] in the RBM (468–473) of the Omicron variant, which is required for hACE2 binding. This transition is significant in terms of the effect of disordered residues/regions on spike protein stability and binding to ACE2.[18]

3.4 | Protein structure analysis

For structural comparison, the protein structures of WT (PDB ID: 6MOJ), Omicron (BA.1) cryo-EM structure (PDB ID: 7T9L), and homology modeled BA.1.1, BA.2, and BA.3 subvariants based on cyro-EM structure (PDB ID: 7T9L) were employed. The structural quality of the homology modeled RBD structures was evaluated using the Ramachandran plot and Errat provided from the SAVES v6.0 web server (https://saves.mbi.ucla.edu/). Ramachandran's plot Analyzes residue-by-residue geometry and overall structural geometry to determine the stereochemical quality of a protein structure. Errat compares statistics from highly refined structures to the statistics of nonbonded interactions between distinct atom types and graphs the value of the error function vs location of a nine-residue sliding window. In the Ramachandran plot, the homology modeled of RBD of BA.2 and BA.3 showed residues in most preferred areas with 90.2% and residues in extra permitted regions with 9.8%. BA.2 and BA.3 both have an Errat score of 89.4. This demonstrates that the overall RBD protein structure of BA.2 and BA.3 is reliable. TM-align tool generates optimum residue-to-residue alignment based on structural similarity using heuristic dynamic programming iterations; scores greater than 0.5 presume the same fold in general. Based on TM-align findings, the RMSD value for all BA.1, BA.1.1, BA.2, and BA.3 is 0.68 based on superposition with WT. This reveals that Omicron (BA.1, BA.2, and BA.3) have the same structural topology and fold as the WT. Geometric and topological properties of protein structures, including surface pockets, interior cavities, and cross channels, are of fundamental importance for proteins to carry out their functions. The binding pocket shown in solvent accessible surface area and volume was predicted for WT and for Omicron (BA.1, BA.2, and BA.3) using CASTp 3.0. The binding pocket of WT area is 73.39 and volume is 60.83. For both BA.1 and BA.1.1, the calculated area is 93.87 and volume is 37.52. For BA.2, the predicted area is 49.03 and calculated volume is 16.44. For BA.3, the predicted area is 49.03 and volume predicted is 16.43. From the analysis binding pocket area increased for BA.1 than WT, while BA.2 and BA.3 decreased whereas binding pocket volume decreases for all BA.1, BA.2, and BA.3 than WT. We observed that the positive electrostatic surface potential of Omicron and sub-variants is significantly increased as per the previous study reported.[41] In the RBD, BA.2 and BA.3 observed to have higher positive electrostatic potential (EP) than BA.1.1, BA.1, and WT. This may facilitate RBD interaction with the negatively charged ACE2, hence enhancing the ACE2 receptor's affinity (Figure 3A–F). While the spike (S) protein's NTD has a high electronegative EP (Figure 3G–K), in the NTD of BA.2 and BA.3 has higher electronegative EP than BA.1.1, BA.1, and ET. Instead of influencing the RBD-ACE2 interaction, the S protein-NTD could play a role in viral binding to another component of the host cell surface. The NTD domain of SARS-CoV-2 has been shown to recognize and bind to a wide range of host receptors and candidate co-receptors. If EP positive for SARS-CoV-2 receptor binding is significant, as it is for RBD-ACE2 interaction, then the negative EP of NTD value indicates that the Omicron variant binds receptors less efficiently than the WT. Given that at least one receptor is highly expressed in lung and bronchial cells, the EP of NTD negative value could be one of the factors contributing to why the Omicron variant is thought to be less harmful to the lower respiratory tract.[42] Each of these modifications has the potential to affect viral pathogenicity, infectivity, and transmission.[43]

3.5 | Pathogenicity and molecular docking

The protein sequences were submitted to PredictSNP to predict the effects of mutations on protein function for Omicron SARS-CoV-2 S and hACE2. PredictSNP was used to examine the functional modifications and predictions of the tolerated and deleterious nsSNPs. Our data revealed that among a total of 45 mutations, 39 were neutral, and 6 were deleterious with regard to pathogenicity. Y505H, N786K predicted to be deleterious BA.1, BA.1.1, BA.2, and BA.3. T95I, N211I, and V213R mutations are predicted to be deleterious in BA.1, BA.1.1, and BA.3. N856K mutations are predicted to be deleterious in BA.1 and BA.1.1 (Table 1).

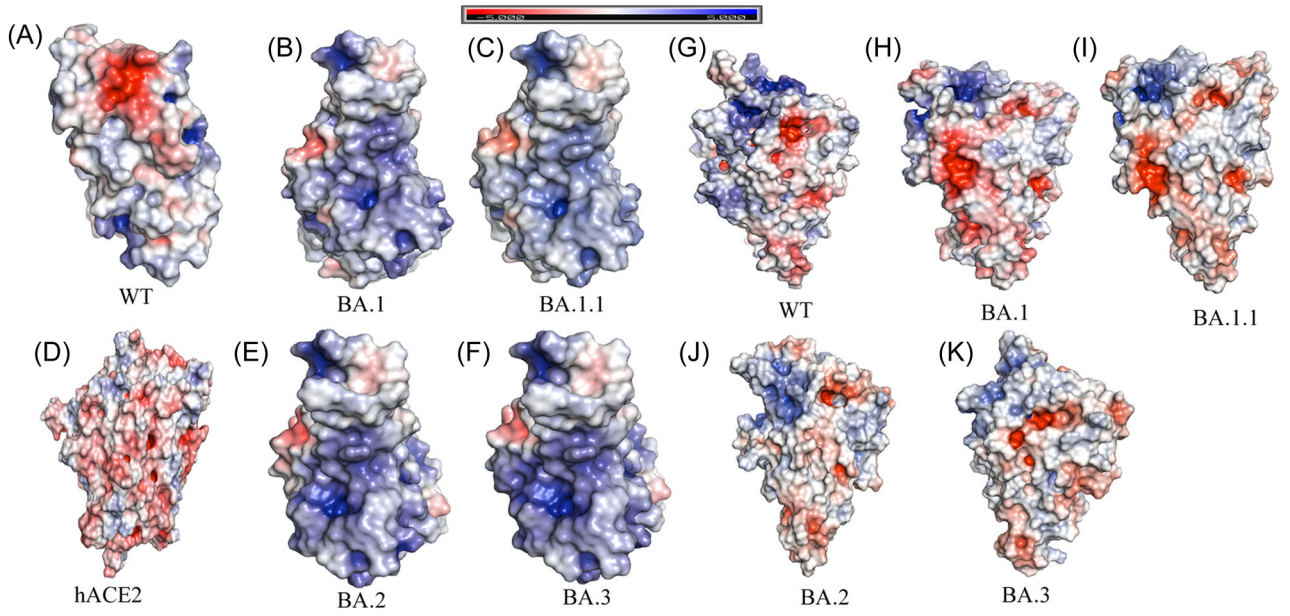

FIGURE 3 Comparison between the wild-type (WT) (A), Omicron variants: BA.1 (B), BA.1.1 (C), BA.2 (E), and BA.3 (F) spike receptor-binding domains (RBDs) and shown human ACE2 (D). Electrostatic potential of N-terminal doman (NTD) of spike protein: WT (G), BA.1 (H), BA.1.1 (I), BA.2 (J), and BA.3 (K). Protein surface is colored according to the electrostatic potential shown in top view. Color scale ranges from −5 kT/e (red) to +5 kT/e (blue) as reported by the bar at the top. The human ACE2 show electronegative potential while Omicron variant of RBD shows there is an increase of electropositive electrostatic potential when compared to WT, while NTD shows increase in electronegative electrostatic potential.

The interaction with the SARS-CoV-2 virus's Spike protein RBD and the ACE2 cell surface protein was required for viral infection of cells. The virus increases its evolutionary advantages at the RBD by introducing changes that increase the ACE2-RBD binding affinity or that enable it to avoid antibody detection.[44] Because the virus's infectivity in human cells has been improved, any one mutation is unlikely to result in a large increase in viral infectivity. Multiple RBD mutations increase infectivity, which seems to be the case with Omicron, and so appears to be a viable infection pathway. The protein–protein docking method was used, and both HawkDock server and the cluspro docking server were used. The PDB (6M0J) crystal structure of the SARS-CoV-2 spike RBD associated with ACE2 for WT, as well as the Cryo-EM structure of BA.1 (PDB ID:7T9l) and homology models of BA.2 and BA.3, were used in this investigation.

RBD-ACE2 docking was performed to identify binding pockets and interacting residues using the HawkDock protein–protein docking server. It integrates the ATTRACT docking algorithm, the HawkRank scoring function, and the MM/GBSA free energy decomposition analysis for binding free energy calculations. As shown in Figure 4, binding free energy complex for WT is −37.44 (kcal/mol). According to HawkDock server, BA.3 (−73.55) has the highest binding free energy compared to BA.2 (−72.36), BA1.1 (−71.56), and BA.1 (−70.6).

The RBD of SARS-CoV-2 was extracted from hACE2 and utilized for protein–protein docking in the WT and BA.1. After each docking between hACE2 and S protein of each variant, 30 cluster models had been created, of which the model with lowest energy score was selected. The selected cluster models were downloaded in PDB format for further analysis. The homology model is docked with hACE2 for BA.2 and BA.3. The docking energy of WT is −799.6 with hACE2, the docking energy of BA.1 is −943.4 with hACE2, the docking energy for BA.1.1 is −946.8, the docking energy of BA.2 is −974.0 with hACE2, and the docking energy of BA.3 is −999.3 with hACE2. Docking results show that BA.1, BA1.1, BA.2, and BA.3 have a greater affinity for hACE2 than WT, implying that it has a higher potential for transmission than WT. We observed among Omicron, BA.2 and BA.3 have a higher affinity for hACE2 than WT and BA.1, indicating that they had a higher potential for transmission than BA.1 based on both protein–protein docking servers.

In addition, the effect of each point mutation residue of RBM on interaction with hACE2 was studied. Among the common mutations in RBM shared by BA.1, BA.1.1, BA.2, and BA.3, Q493R (−581.53), N501Y (−560.81), Q498 (−527.38), T478K (−517.03), and Y505H had the highest binding affinity with hACE2 (−502.24). Furthermore, the Omicron variant with "Q498R-N501Y" double mutations may enhance RBD binding affinity to the hACE2 receptor. However, the point mutations N440k (−496.38) and E484 (−478.49) had the lowest binding affinity. BA.1 unique mutation G496S (−505.58) has the highest binding affinity. BA.2 unique mutation D405N (−487.86) has the lowest binding affinity with hACE2. Previous research indicated that the N501Y mutation identified in the RBD region increased protein stability as well as a stronger affinity to human ACE2 protein,[45] which has the potential to increase infectivity and

TABLE 1 The predicted effect of Spike protein single mutations of Omicron variants on pathogenicity by using PredictSNP tool.

Wild residue	Position	Target residue	Predicted type	Predict SNP accuracy	Mutation present in
T	19	I	NEUTRAL	65%	BA.2
A	27	S	NEUTRAL	82%	BA.2
A	67	V	NEUTRAL	73%	BA.1, BA.1.1
T	**95**	**I**	**DELETERIOUS**	**60%**	**BA.1, BA.1.1, BA.3**
G	142	D	NEUTRAL	74%	BA.1, BA.1.1, BA.3
Y	144	D	NEUTRAL	74%	BA.1, BA.1.1
Y	145	D	NEUTRAL	63%	BA.1, BA.1.1
N	**211**	**I**	**DELETERIOUS**	**60%**	**BA.1, BA.1.1, BA.3**
L	212	V	NEUTRAL	82%	BA.1, BA.1.1, BA.3
V	**213**	**R**	**DELETERIOUS**	**65%**	**BA.1, BA.1.1, BA.3**
R	214	E	NEUTRAL	75%	BA.1.1
G	339	D	NEUTRAL	73%	BA.1, BA.1.1, BA.2, BA.3
R	346	K	NEUTRAL	82%	BA.1.1
S	371	L	NEUTRAL	82%	BA.1, BA.1.1, BA.3
S	371	F	NEUTRAL	73%	BA.2
S	373	P	NEUTRAL	82%	BA.1, BA.1.1, BA.2, BA.3
S	375	F	NEUTRAL	75%	BA.1, BA.1.1, BA.2, BA.3
T	376	A	NEUTRAL	65%	BA.2
D	405	N	NEUTRAL	62%	BA.2, BA.3
R	408	S	NEUTRAL	73%	BA.2
K	417	N	NEUTRAL	73%	BA.1, BA.1.1, BA.2, BA.3
N	440	K	NEUTRAL	73%	BA.1, BA.1.1, BA.2, BA.3
G	446	S	NEUTRAL	82%	BA.1, BA.1.1, BA.3
S	477	N	NEUTRAL	82%	BA.1, BA.1.1, BA.2, BA.3
T	478	K	NEUTRAL	63%	BA.1, BA.1.1, BA.2, BA.3
E	484	A	NEUTRAL	82%	BA.1, BA.1.1, BA.2, BA.3
Q	493	R	NEUTRAL	75%	BA.1, BA.1.1, BA.2, BA.3
G	496	S	NEUTRAL	63%	BA.1, BA.1.1
Q	498	R	NEUTRAL	68%	BA.1, BA.1.1, BA.2, BA.3
N	501	Y	NEUTRAL	60%	BA.1, BA.1.1, BA.2, BA.3
Y	**505**	**H**	**DELETERIOUS**	**60%**	**BA.1, BA.1.1, BA.2, BA.3**

TABLE 1 (Continued)

Wild residue	Position	Target residue	Predicted type	Predict SNP accuracy	Mutation present in
T	547	K	NEUTRAL	82%	BA.1, BA.1.1
D	614	G	NEUTRAL	82%	BA.1, BA.1.1, BA.2, BA.3
H	655	Y	NEUTRAL	73%	BA.1, BA.1.1, BA.2, BA.3
N	679	H	NEUTRAL	82%	BA.1, BA.1.1, BA.2, BA.3
N	679	K	NEUTRAL	82%	BA.3
P	681	K	NEUTRAL	82%	BA.1, BA.1.1, BA.2, BA.3
N	**764**	**K**	**DELETERIOUS**	**71%**	**BA.1, BA.1.1, BA.2, BA.3**
D	796	Y	NEUTRAL	75%	BA.1, BA.1.1, BA.2, BA.3
N	**856**	**K**	**DELETERIOUS**	**75%**	**BA.1, BA.1.1**
Q	954	H	NEUTRAL	73%	BA.1, BA.1.1, BA.2, BA.3
N	969	K	DELETERIOUS	54%	BA.1, BA.1.1, BA.2, BA.3
L	981	F	NEUTRAL	82%	BA.1, BA.1.1

Note: Predicted deleterious mutation marked as bold.

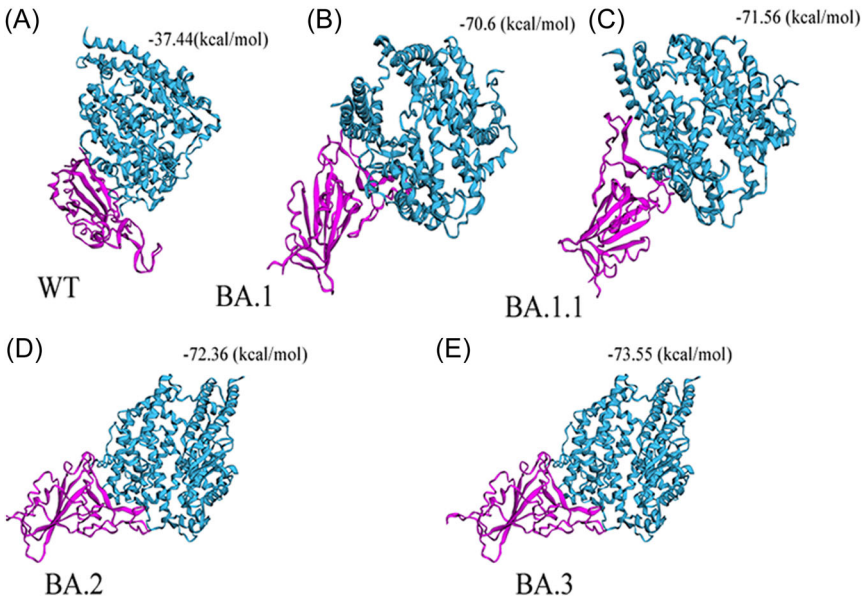

FIGURE 4 Docking between (A) wild-type (WT)-RBD (B) Omicron BA.1-RBD, and (C) Omicron BA.1.1-RBD (D) Omicron BA.2-RBD (E) Omicron BA.3-RBD with hACE2. Based on docking energy it shows Omicron BA.2 and BA.3-RBD have a high binding affinity with hACE2 compared to Omicron variant BA.1, B.1.1, and WT. Docking scores are shown in MM/GBSA free energy decomposition analysis for binding free energy calculations at the top of each variant. hACE2, human angiotensin I-converting enzyme 2; RBD, receptor-binding domain.

transmission. Despite its location in RBD, S477N exhibits a decreased affinity for the host cell.[46] Interactions involving Omicron variant mutations at residues 493, 496, 498, and 501 seem to restore ACE2 binding efficiency lost owing to other changes such as K417N (Table 2). The retention of total ACE2 binding affinity for the Omicron spike protein shows that compensatory mutations exist that restore increased ACE2 affinity. Omicron has a similar triple mutation like beta variant, "K417N + E484A + N501Y," which may result in immune escape.[47]

At residue K417, the WT forms a salt bridge and a hydrogen bond. Cryo-EM structural study of the Omicron variant (BA.1) spike protein in complex with human ACE2 shows new salt bridges and hydrogen bonds produced by R493, R498 mutated residues in the RBD with ACE2. From PISA analysis (Table 3), we predicted that new salt bridges and hydrogen

TABLE 2 Docking analysis of single-point mutation of Wuhan-RBM (receptor-binding motif), Omicron (BA.1)-RBD, and sub-variants (BA1.1, BA.2, and BA.3)-RBD residues with ACE2 using HEX software.

S. No.	Omicron RBM		Docking energy
1	Wild-type	–	−500.37
1	Common mutation shared by BA.1, BA.1.1, BA.2, and BA.3	N440K	−496.38
2		S477N	−500.05
3		T478K	−517.03
4		T478K	−478.49
5		E484A	−581.53
6		Q493R	−527.38
7		Q498R	−560.81
8		N501Y	−502.24
9	Unique mutation BA.1	Y505H	−505.58
10	Unique mutation BA.2	D405N	−487.86

TABLE 3 The salt bridge formation and hydrogen bond formation between ACE2-RBD predicted for Omicron and sub-variants using PDBePISA (PISA) web-based tool.

	Salt bridge formation (ACE2-RBD)	Hydrogen bond formation (ACE2-RBD)
WT[a]	**ASP 30-Lys417** (data from publication)	Gln24-Asn487
(PDB ID: 6MOJ)		**Asp30-Lys417**
		Glu35-Gln493
		Glu37-Tyr505
		Asp38-Tyr449
		Tyr41-Thr500
		Tyr41-Asn501
		Gln42-Gly446
		Gln42-Tyr449
		Tyr83-Tyr489
		Tyr83-Asn487
		Gly502-Lys353
		Tyr505-Arg393
BA.1[a]	**GLU 35-ARG 493**	ASP 38-TYR 449
(PDB I D:7T9L)	**ASP 38-ARG 498**	ASP 38-TYR 449
		GLN 42-TYR 449
		TYR 83-TYR 489
		GLU 35-ARG 493
		ASP 38-SER 496
		ASP 38-ARG 498
		GLN 42-ARG 498
		TYR 41-THR 500
		LYS 353-GLY 502
		HIS 34-TYR 453
		TYR 83-ASN 487
		LYS 353-SER 496
		TYR 41-THR 500
		LYS 353-TYR 501
BA.1.1	**GLU 57-LYS 478**	LYS 31-TYR 450
	GLU 35-ARG 490	LYS 68-TYR 470
	GLU 35-ARG 493	GLN 42-ALA 481
	ASP 38-ARG 490	GLN 42-CYS 485
	ASP 30-ARG 495	THR 27-THR 497
	ASP 30-ARG 498	ASP 30-TYR 446
		ASN 61-ASN 474
		GLU 57-ASN 474
		GLU 57-ASN 474
		GLU 57-LYS 478
		GLN 42-ASN 484
		ASN 61-ASN 484
		LEU 39-TYR 486
		GLU 35-ARG 493
		ASP 38-ARG 490
		ASP 30-ARG 498
BA.2	ASP 30-ARG 490	ARG 559-ALA 472
	ASP 30-ARG 490	GLN 388-ASN 484
	GLU 35-ARG 495	LYS 68-THR 497
	ASP 38-HIS 502	**ASP 30-ARG 490**
	ASP 38-ARG 400	**GLU 35-ARG 495**
		ASP 38-ARG 400
		LYS 353-ASN 414
		ALA 387-TYR 486
BA.3	**GLU 35-HIS 499**	GLN 24-ALA 469
	GLU 35-ARG 397	LYS 31-TYR 447
	GLU 75-ARG 487	GLN 42-TYR 495

(Continues)

TABLE 3 (Continued)

	Salt bridge formation (ACE2-RBD)	Hydrogen bond formation (ACE2-RBD)
		LYS 68-THR 494
		HIS 34-ARG 397
		ASP 38-VAL 497
		ASP 38-GLY 498
		ASP 38-HIS 499

[a]Data from publication.[18,19]

bond formation for mutated residues in BA.1.1 (K478), BA.2 (R400, R490, and R495), and BA.3 (R397 and H499).

4 | CONCLUSION

In this study, Omicron (BA.1) and sub-variants (BA.1.1, BA.2, and BA.3) are compared and investigated with WT using various computational tools. There are 11 shared common mutations G339D, S373P, S375F, K417N, N440K, S477N, T478K, E484A, Q493R, Q498R, and N501Y in RBD Omicron and sub-variants that may contribute significantly to changing the host spectrum of SARS-CoV-2 in immune evasion and potential transmission. The Omicron sub-variants (BA.1.1, BA.2 and BA.3) are likely more transmissible than omicron (BA.1) and Delta. Even if early data indicate that an Omicron infection is less severe than a Delta infection, the quick rise in cases will result in an increase in hospitalizations, placing strain on health care systems to treat individuals with both COVID-19 and other forms of disease. Even though Omicron sub-variants are predicted to be highly transmissible, we anticipate that future COVID-19 waves may be controlled by updated vaccines, reduced vaccine inequity, improved antiviral therapy, and preventative actions taken by the susceptible population.

5 | LIMITATIONS OF THE STUDY

This evaluation of Omicron variants was mostly confined to computational sequence and structural predictions, and these results should be investigated and validated in future experiments. This study revealed fundamental information about the Omicron protein structures, laying the framework for future research on the SARS-CoV-2 Omicron and sub-variants.

AUTHOR CONTRIBUTIONS

Conceptualization, investigation, writing – original draft preparation: Suresh Kumar. *Writing – review and editing*: Kalimuthu Karuppanan and Gunasekaran Subramaniam. *Data curation and formal analysis*: Suresh Kumar. *Methodology, data curation, investigation, and validation*: Suresh Kumar, Kalimuthu Karuppanan, and Gunasekaran Subramaniam. *Project administration, and supervision*: Suresh Kumar.

ACKNOWLEDGMENTS

The authors acknowledge the Faculty of Health and Life Sciences, Management and Science University, Malaysia; Division of Cardiovascular Medicine, Radcliffe Department of Medicine, Wellcome Centre for Human Genetics, University of Oxford, Oxford, UK and Department of Physiology, Anatomy, and Genetics, University of Oxford, Oxford, UK. The authors also acknowledge GISAID (https://www.gisaid.org/) for facilitating open data sharing.

CONFLICT OF INTEREST

The authors declare no conflict of interest.

DATA AVAILABILITY STATEMENT

Data sharing is not applicable to this article as no new data were created or analyzed in this study.

ORCID

Suresh Kumar http://orcid.org/0000-0001-5682-0938

REFERENCES

1. Ludwig S, Zarbock A. Coronaviruses and SARS-CoV-2: a brief overview. *Anesth Analg*. 2020;131(1):93-96.
2. Wang L, Cheng G. Sequence analysis of the emerging SARS-CoV-2 variant Omicron in South Africa. *J Med Virol*. 2022;94(4):1728-1733
3. He X, Hong W, Pan X, Lu G, Wei X. SARS-CoV-2 omicron variant: characteristics and prevention. *MedComm*. 2021;2(4):838-845.
4. Fantini J, Yahi N, Colson P, Chahinian H, La Scola B, Raoult D. The puzzling mutational landscape of the SARS-2-variant Omicron. *J Med Virol*. 2022;94(5):2019-2025.
5. Kumar S. *COVID-19: a drug repurposing and biomarker identification by using comprehensive gene-disease associations through protein-protein interaction network analysis*. *Preprints*. 2020;2020030440.
6. Kumar S. Protein–protein interaction network for the identification of new targets against novel Coronavirus. In: Roy K, ed. *In Silico Modeling of Drugs Against Coronaviruses: Computational Tools and Protocols*. Springer US; 2021:213-230.
7. Kumar S. Online resource and tools for the development of drugs against novel Coronavirus. In: Roy K, ed. *In Silico Modeling of Drugs Against Coronaviruses: Computational Tools and Protocols*. Springer US; 2021:735-759.
8. Kumar SMS, Jia Jin W, Bt Azman NA, et al. *COVID-19 vaccine candidates by identification of B and T cell multi-epitopes against SARS-COV-2*. *Preprints*. 2020;2020080092.
9. Desingu PA, Nagarajan K, Dhama K. Emergence of Omicron third lineage BA.3 and its importance. *J Med Virol*. 2022;94:1808-1810.
10. Colson P, Delerce J, Beye M, et al. First cases of infection with the 21L/BA.2 Omicron variant in Marseille, France. *J Med Virol*. 2022;94:3421-3430.
11. Kumar S, Thambiraja TS, Karuppanan K, Subramaniam G. Omicron and delta variant of SARS-CoV-2: a comparative computational study of spike protein. *J Med Virol*. 2022;94(4):1641-1649.
12. The UniProt Consortium. UniProt: the universal protein knowledgebase. *Nucleic Acids Res*. 2016;45(D1):D158-D169.
13. Sayers EW, Cavanaugh M, Clark K, et al. GenBank. *Nucleic Acids Res*. 2020;49(D1):D92-D96.
14. Bogner P, Capua I, Lipman DJ, Cox NJ. A global initiative on sharing avian flu data. *Nature*. 2006;442(7106):981.
15. Sievers F, Higgins DG. Clustal omega. *Curr Protoc Bioinform*. 2014;48(1):3.13.11-13.13.16.

16. Gasteiger E, Gattiker A, Hoogland C, Ivanyi I, Appel RD, Bairoch A. ExPASy: the proteomics server for in-depth protein knowledge and analysis. *Nucleic Acids Res*. 2003;31(13):3784-3788.
17. Sen TZ, Jernigan RL, Garnier J, Kloczkowski A. GOR V server for protein secondary structure prediction. *Bioinformatics*. 2005;21(11):2787-2788.
18. Xu C, Wang Y, Liu C, et al. Conformational dynamics of SARS-CoV-2 trimeric spike glycoprotein in complex with receptor ACE2 revealed by cryo-EM. *Sci Adv*. 2021;7(1):eabe5575.
19. Mannar D, Saville JW, Zhu X, et al. SARS-CoV-2 Omicron variant: antibody evasion and cryo-EM structure of spike protein-ACE2 complex. *Science*. 2022;375:760-764.
20. Waterhouse A, Bertoni M, Bienert S, et al. SWISS-MODEL: homology modelling of protein structures and complexes. *Nucleic Acids Res*. 2018;46(W1):W296-W303.
21. Zhang Y, Skolnick J. TM-align: a protein structure alignment algorithm based on the TM-score. *Nucleic Acids Res*. 2005;33(7):2302-2309.
22. Tian W, Chen C, Lei X, Zhao J, Liang J. CASTp 3.0: computed atlas of surface topography of proteins. *Nucleic Acids Res*. 2018;46(W1):W363-W367.
23. Jurrus E, Engel D, Star K, et al. Improvements to the APBS biomolecular solvation software suite. *Prot Sci*. 2018;27(1):112-128.
24. Weng G, Wang E, Wang Z, et al. HawkDock: a web server to predict and analyze the protein–protein complex based on computational docking and MM/GBSA. *Nucleic Acids Res*. 2019;47(W1):W322-W330.
25. Macindoe G, Mavridis L, Venkatraman V, Devignes M-D, Ritchie D. HexServer: an FFT-based protein docking server powered by graphics processors. *Nucleic Acids Res*. 2010;38:W445-W449.
26. Bendl J, Stourac J, Salanda O, et al. PredictSNP: robust and accurate consensus classifier for prediction of disease-related mutations. *PLoS Comput Biol*. 2014;10(1):e1003440.
27. Hassanzadeh K, Perez Pena H, Dragotto J, et al. Considerations around the SARS-CoV-2 spike protein with particular attention to COVID-19 brain infection and neurological symptoms. *ACS Chem Neurosci*. 2020;11(15):2361-2369.
28. Almofti YA, Abd-Elrahman KA, Eltilib EEM. Vaccinomic approach for novel multi epitopes vaccine against severe acute respiratory syndrome coronavirus-2 (SARS-CoV-2). *BMC Immunol*. 2021;22(1):22.
29. Cui Z, Liu P, Wang N, et al. Structural and functional characterizations of infectivity and immune evasion of SARS-CoV-2 Omicron. *Cell*. 2022;185:860-871.
30. Basu S, Mukhopadhyay S, Das R, Mukhopadhyay S, Singh PK, Ganguli S. *Impact of clade specific mutations on structural fidelity of SARS-CoV-2 proteins*. *bioRxiv*. 2020. doi:10.1101/2020.10.20.347021
31. Socher E, Conrad M, Heger L, et al. Mutations in the B.1.1.7 SARS-CoV-2 spike protein reduce receptor-binding affinity and induce a flexible link to the fusion peptide. *Biomedicines*. 2021;9(5):1-13.
32. Meng B, Ferreira IATM, Abdullahi A, et al. *SARS-CoV-2 Omicron spike mediated immune escape and tropism shift*. *bioRxiv*. 2022. doi:10.1101/2021.12.17.473248
33. Suthar MS, Zimmerman MG, Kauffman RC, et al. Rapid generation of neutralizing antibody responses in COVID-19 patients. *Cell Rep Med*. 2020;1(3):100040.
34. Cerutti G, Guo Y, Zhou T, et al. Potent SARS-CoV-2 neutralizing antibodies directed against spike N-terminal domain target a single supersite. *Cell Host Microbe*. 2021;29(5):819-833.
35. Han P, Li L, Liu S, et al. Receptor binding and complex structures of human ACE2 to spike RBD from omicron and delta SARS-CoV-2. *Cell*. 2022;185:630-640.
36. Meng B, Kemp SA, Papa G, et al. Recurrent emergence of SARS-CoV-2 spike deletion H69/V70 and its role in the Alpha variant B.1.1.7. *Cell Rep*. 2021;35(13):109292.
37. Li A, Maier A, Carter M, Guan TH. Omicron and S-gene target failure cases in the highest COVID-19 case rate region in Canada-December 2021. *J Med Virol*. 2022;94(5):1784-1786.
38. Abrusán G, Marsh JA. Alpha helices are more robust to mutations than beta strands. *PLoS Comput Biol*. 2016;12(12):e1005242.
39. Williams JK, Wang B, Sam A, Hoop CL, Case DA, Baum J. Molecular dynamics analysis of a flexible loop at the binding interface of the SARS-CoV-2 spike protein receptor-binding domain. *Proteins*. 2022;90:1044-1053.
40. Mendoza-Espinosa P, García-González V, Moreno A, Castillo R, Mas-Oliva J. Disorder-to-order conformational transitions in protein structure and its relationship to disease. *Mol Cell Biochem*. 2009;330(1-2):105-120.
41. Pascarella S, Ciccozzi M, Bianchi M, Benvenuto D, Cauda R, Cassone A. The electrostatic potential of the Omicron variant spike is higher than in Delta and Delta-plus variants: a hint to higher transmissibility? *J Med Virol*. 2022;94:1277-1280.
42. Pascarella S, Ciccozzi M, Bianchi M, Benvenuto D, Cauda R, Cassone A. The value of electrostatic potentials of the spike receptor binding and N-terminal domains in addressing transmissibility and infectivity of SARS-CoV-2 variants of concern. *J Infect*. 2022;84(5):e62-e63.
43. Fantini J, Yahi N, Azzaz F, Chahinian H. Structural dynamics of SARS-CoV-2 variants: a health monitoring strategy for anticipating Covid-19 outbreaks. *J Infect*. 2021;83(2):197-206.
44. Shang J, Ye G, Shi K, et al. Structural basis of receptor recognition by SARS-CoV-2. *Nature*. 2020;581(7807):221-224.
45. Tian F, Tong B, Sun L, et al. N501Y mutation of spike protein in SARS-CoV-2 strengthens its binding to receptor ACE2. *eLife*. 2021;10:10.
46. Mathavan S, Kumar S. Evaluation of the effect of D614g, N501y and S477n mutation in Sars-Cov-2 through computational approach. Preprints.org; 2020.
47. Tian D, Sun Y, Xu H, Ye Q. The emergence and epidemic characteristics of the highly mutated SARS-CoV-2 Omicron variant. *J Med Virol*. 2022;94(6):2376-2383.

SUPPORTING INFORMATION

Additional supporting information can be found online in the Supporting Information section at the end of this article.

How to cite this article: Kumar S, Karuppanan K, Subramaniam G. Omicron (BA.1) and sub-variants (BA.1.1, BA.2, and BA.3) of SARS-CoV-2 spike infectivity and pathogenicity: A comparative sequence and structural-based computational assessment. *J Med Virol*. 2022;94:4780-4791. doi:10.1002/jmv.27927